Available online at www.sciencedirect.com

ScienceDirect

Mendeleev Commun., 2024, **34**, 492–495

Mendeleev Communications

Nanosized systems of aluminum phthalocyanine and amphiphilic copolymers of *N*-vinylpyrrolidone with mono- and dimethacrylates for photodynamic therapy and fluorescence diagnostics

Svetlana V. Kurmaz,* Ivan V. Ulyanov, Nina S. Emelyanova, Vladimir A. Kurmaz, Alexey V. Kozlov, Lev R. Sizov and Alexander Yu. Rybkin

Federal Research Center of Problems of Chemical Physics and Medicinal Chemistry, Russian Academy of Sciences, 142432 Chernogolovka, Moscow Region, Russian Federation. E-mail: skurmaz@icp.ac.ru

DOI: 10.1016/j.mencom.2024.06.007

Water-soluble nanosized systems of aluminum phthalocyanine, which is a promising photosensitizer for photodynamic therapy and fluorescence diagnostics, were obtained by encapsulating it in biocompatible copolymers of *N*-vinylpyrrolidone with mono- and dimethacrylates. The physicochemical (water solubility, stability and size of nanoparticles) and photophysical (absorption and fluorescence) properties of the resulting nanoparticles in aqueous solution were determined. Quantum chemical modeling revealed the formation of coordination bonds between the Al atom of the dye and the oxygen atoms of all monomer units.

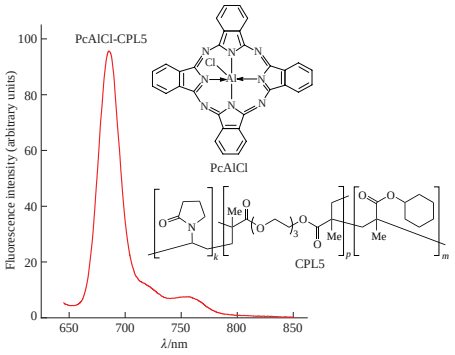

Keywords: *N*-vinylpyrrolidone, dimethacrylates, terpolymer, aluminum phthalocyanine, encapsulation, fluorescence, quantum chemical modeling.

Being structurally close to the widely used metal complexes of porphyrins, metal complexes of phthalocyanines are much more accessible in preparation and convenient in practice.[1] Therefore, the scope of their application is even wider, from chemical, photo- and electrochemical catalysis to current sources, supercapacitors, sensors, electrochromic devices, information storage, optoelectronics, solar cells, photosensitizers (PSs) for photodynamic therapy (PDT), *etc.*[1–5] PDT is an effective non-invasive method for the treatment of oncological and infectious diseases, which uses non-toxic drugs acting as PSs. The fluorescence of the PS and its ability to selectively accumulate in tumor tissues make it possible to diagnose the formation of tumors in the early stages and determine their boundaries. When such a non-toxic PS is excited by light, it produces highly toxic reactive oxygen species that cause the death of cancer cells without destroying healthy tissues. Phthalocyanines are promising candidates for PSs in PDT due to their high molar absorption coeffcient ($\log \varepsilon \sim 5$) in the red region of the spectrum (650–700 nm), high photostability and low dark toxicity.[6] In clinical practice, PSs are divided into first (hematoporphyrin derivatives) and second (chlorins, porphyrins and phthalocyanines) generations.[3] However, most of them are poorly soluble in physiological media, have unfavorable pharmacokinetics and low tumor selectivity. To solve these problems, third-generation PSs are being actively developed, which are known second-generation PSs in combination with various delivery systems (lipids, lipoproteins, polymers, *etc.*).[3,7–9] The inclusion of the active substance in the carrier will help reduce the toxic effect by reducing its dose, and will also protect it from contact with healthy tissues of the body. Currently, several types of nanoparticles (NPs) loaded with second-generation PSs are approved for clinical application. For example, the drug 'Photolon' (a complex of trisodium salt of chlorin e_6 with low molecular weight poly-*N*-vinylpyrrolidone), which has a higher selectivity of accumulation in the tumor and a more effective photodynamic effect compared to the native dye, has been approved as a drug for PDT of a number of tumors.[10]

Dendritic polymers are very promising platforms for the delivery of PSs,[11–13] which are capable of imparting water solubility to even highly hydrophobic dyes. Hyperbranched copolymers of *N*-vinylpyrrolidone (VP) with mono- and dimethacrylates are effective encapsulation agents for various types of biologically active hydrophobic compounds[14–18] and can be a useful tool for the preparation of water-soluble third-generation PSs. Previously, we obtained polymeric NPs with hydrophobic methyl pheophorbide *a* (a derivative of chlorin e_6) based on amphiphilic dendritic copolymers of VP with mono- and dimethacrylates[13] and studied their phototoxic effect in HeLa cells, which was 1.5–2 times higher than that of the native chlorin e_6 trisodium salt, one of the most effective PSs used in clinical practice.

The monomeric aluminum phthalocyanine, PcAlCl [Figure 1(*a*)], exhibits high photostability, strong absorption in the region of 650–680 nm (in the so-called 'therapeutic window') and a high quantum yield of singlet oxygen; its sulfo substituted derivative 'Photosens' is used as a second-generation PS in PDT and fluorescence diagnostics.[3,19,20] However, the use of PcAlCl is limited due to its high hydrophobic properties and tendency to aggregate in aqueous solutions with the formation of dimeric H- and J-aggregates.

© 2024 Mendeleev Communications. Published by ELSEVIER B.V. on behalf of the N. D. Zelinsky Institute of Organic Chemistry of the Russian Academy of Sciences.

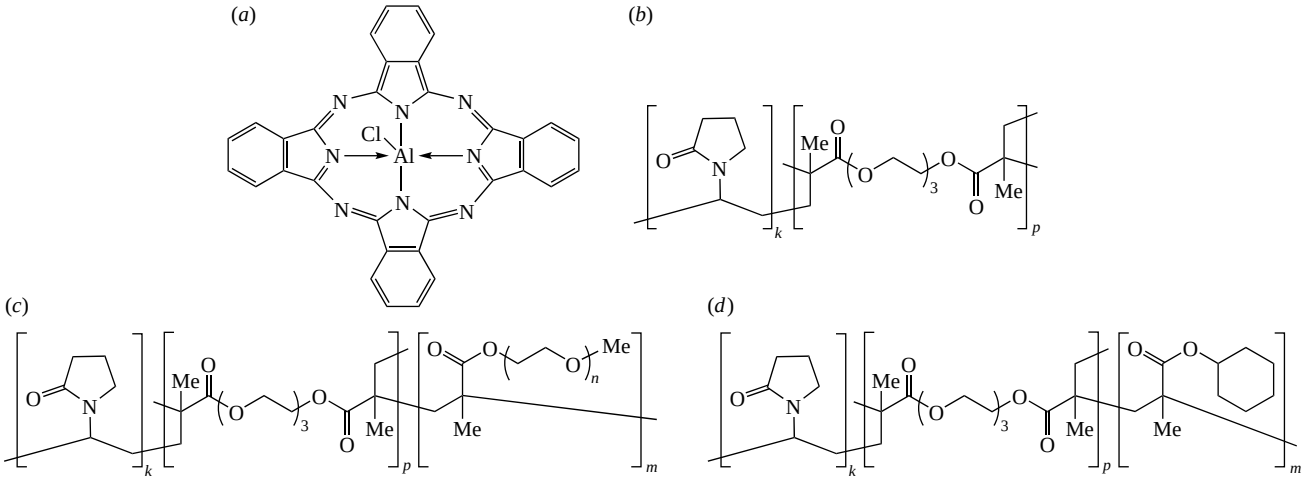

Figure 1 Chemical structures of (*a*) PcAlCl, (*b*) VP–TEGDM copolymer (CPL1), (*c*) VP–PEGMEM–TEGDM terpolymers (CPL2, CPL3 and CPL4) with different monomer ratios ($n \sim 8$) and (*d*) VP–(cyclo-HMA)–TEGDM terpolymer (CPL5).

The purpose of this work was to develop nanosized systems with PcAlCl encapsulated in various VP copolymers with mono- and dimethacrylates for PDT and fluorescence diagnostics, to study their physicochemical (water solubility, stability and NP size) and photophysical (absorption and fluorescence) properties depending on the type of polymer matrix, and also to carry out quantum chemical modeling of the structure of the complex between the PcAlCl molecule and the monomer units of copolymers.

To encapsulate the dye, we used the VP–TEGDM copolymer (CPL1), as well as the VP–PEGMEM–TEGDM (CPL2, CPL3 and CPL4) and VP–(cyclo-HMA)–TEGDM (CPL5) terpolymers, where TEGDM, PEGMEM and cyclo-HMA are triethylene glycol dimethacrylate, polyethylene glycol methyl ether methacrylate and cyclohexyl methacrylate, respectively, with PEGMEM and cyclo-HMA acting as modifiers of CPL1. The procedure for the synthesis and isolation of copolymers is presented in Online Supplementary Materials and described in detail in published works.[12,13,17] We previously studied the biocompatibility of VP copolymers and found that CPL4 accumulated efficiently in Vero and HeLa cells and had low cytotoxicity.[8]

Figure 1(*b*)–(*d*) shows the structural formulas of the copolymers, while their compositions as well as main physicochemical characteristics such as absolute weight-average molecular weights M_w and average hydrodynamic radii R_h are presented in Table S1 (see Online Supplementary Materials). It can be seen that the content of mono- and dimethacrylate units in the copolymers varies from 5 to 11 mol%, and the molecular weight changes by an order of magnitude. Terpolymers CPL2, CPL4 and CPL5, obtained in the presence of a high concentration of TEGDM, have a high molecular weight and are characterized by a high molecular packing density due to their branched structure. The sulfur content in CPL3 obtained in the presence of 1-decanethiol was 1.6 mol%. The amphiphilicity of terpolymers is determined by their chemical composition and the critical concentration of aggregation of copolymers in water can be used to evaluate it. This value, determined from dynamic light scattering (DLS) data, *i.e.*, according to the dependence of the light scattering intensity on the concentration of the terpolymer in water, was 1.8 and 0.55 mg ml^{-1} for CPL3 and CPL5, respectively. Their macromolecules formed aggregates in aqueous media at significantly lower concentrations than other copolymers. As a consequence, in aqueous solutions of all copolymers, the DLS method revealed both individual macromolecules with hydrodynamic radii $R_h \sim 2$–5 nm and their aggregates, NPs with $R_h \leqslant 30$–100 nm (see Table S1).

The process of encapsulation of PcAlCl into copolymers (for the procedure, see Online Supplementary Materials) is based on the mechanism of intermolecular association resulting from the physical capture of dye molecules by the polymer matrix with their penetration into the internal cavities of the NPs. Hydrophobic interactions between PcAlCl molecules and low-polar regions of polymer chains stimulate the penetration of 'guest' molecules into NPs.

To determine the PcAlCl content in polymer compositions, we recorded the absorption spectra of the native dye in DMSO (see Figure S1), where characteristic absorption bands were observed. In the ultraviolet region there is a Soret absorption band with a maximum at $\lambda = 360$ nm and a Q-band in the red region, the position of which strongly depends on the nature of the solvent.[21] For example, it shifts from 675 nm in low-polar THF to 681 nm in polar DMSO as a result of solvatochromic effect, as well as the binding of the solvent to the Al^{III} ion to form a PcAlCl–solvent complex.[21] In the visible region of the spectrum of PcAlCl in DMSO, a Q absorption band is observed with a maximum at $\lambda = 683$ nm, a shoulder at about 654 nm and a low-intensity absorption band at $\lambda \sim 607$ nm, which correspond to two vibronic transitions characteristic of phthalocyanine metal complexes. The molar extinction coefficient of the absorption band at 683 nm was determined from the dependence of its optical density on the concentration of PcAlCl in DMSO (Figure S1, inset). Then the dry powders of the PcAlCl compositions were dissolved in DMSO, their absorption spectra were recorded (Figure S2) and the optical density value at the maximum of the Q-band peak was measured to determine the concentration of the dye in DMSO, as well as its content in the polymer compositions and the efficiency of its encapsulation (Table 1).

The formation of PcAlCl–copolymer nanostructures in an aqueous solution was confirmed by absorption spectra [Figure 2(*a*)]. A broadening of the Q band, a decrease in its intensity and a shift to shorter wavelengths were observed, which indicates the formation of H- and J-aggregates.

In the series of PcAlCl–terpolymer compositions based on CPL2, CPL3 and CPL4, the maximum intensity of the absorption band related to the monomeric form of PcAlCl is observed for PcAlCl–CPL3 at 683 nm, and the minimum for PcAlCl–CPL4 at 687 nm. In an aqueous solution of PcAlCl–CPL2, the optical density of the absorption band at 687 nm has an intermediate value. The spectrum of the PcAlCl–CPL5 aqueous solution also has an intense peak in this region. Differences in the optical characteristics of encapsulated PcAlCl may be associated with

Table 1 Physicochemical and photophysical characteristics of PcAlCl–CPL compositions and corresponding NPs in water.

PcAlCl–copolymer NPs	PcAlCl content (% dry wt.)	PcAlCl encapsulation efficiency (%)[a]	Absorption Q band λ_{max}/nm	Fluorescence λ_{max}/nm	Relative fluorescence quantum yield Φ_1^{fl}/Φ_2^{fl} (%)[b]
PcAlCl–CPL1	1.31	87.3	687	688	0.34
PcAlCl–CPL2	1.38	92.2	687	688	1.10
PcAlCl–CPL3	1.34	89.4	683	684	3.77
PcAlCl–CPL4	1.37	91.5	687	686	0.80
PcAlCl–CPL5	0.76	86.8	683	685	3.66

[a]The encapsulation efficiency was calculated as the ratio of the mass of encapsulated PcAlCl to the total mass of the dye in the synthesis of PcAlCl–CPL NPs. [b]The fluorescence quantum yield of the standard dye, chlorin e_6 sodium salt, is taken from the published work[22] (Φ^{fl} = 15% in ethanol).

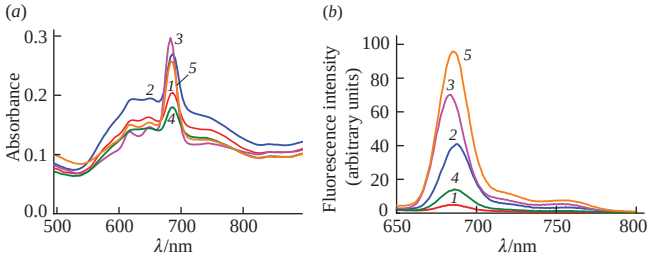

Figure 2 (*a*) Absorption and (*b*) fluorescence spectra of the compositions (*1*) PcAlCl–CPL1, (*2*) PcAlCl–CPL2, (*3*) PcAlCl–CPL3, (*4*) PcAlCl–CPL4 and (*5*) PcAlCl–CPL5 in aqueous solutions. All measurements were carried out at a concentration of PcAlCl–copolymer compositions of 1 mg ml^{-1} using 1 cm quartz cuvette and fluorescence excitation at λ_{ex} = 630 nm.

the localization of dye molecules in regions of different polarity and their aggregation. Apparently, the dye molecules are distributed in areas of NPs enriched in hydrophobic cyclo-HMA units in the case of PcAlCl–CPL5 or hydrophobic $SC_{10}H_{21}$ residues of the chain transfer agent in the case of PcAlCl–CPL3, which leads to the observed decrease in the aggregation of PcAlCl molecules.

This assumption is also supported by fluorescence data of PcAlCl–copolymer compositions in water. It can be seen [Figure 2(*b*)] that the dye encapsulated in CPL5 and CPL3 has the highest fluorescence intensity. In such terpolymer matrices, the aggregation of the dye molecules is significantly reduced, which may be due to the weakening of dye-to-dye intermolecular interactions, as was shown by the example of compositions of another macroheterocyclic dye, methyl pheophorbide *a*, and copolymers of VP with mono- and dimethacrylates in aqueous media.[13] Quantum chemical modeling of such systems showed the possibility of the formation of hydrogen bonds between electron donors in the VP copolymer units and the protons of the dye molecule.

Based on the absorption and fluorescence spectra of aqueous solutions of PcAlCl–copolymer nanostructures, the relative quantum yield of fluorescence was calculated using the sodium salt of chlorin e_6 as a standard dye[22,23] (see Online Supplementary Materials) and its change in the studied series was analyzed. It was shown that PcAlCl encapsulated in terpolymers CPL3 and CPL5 has the highest fluorescence quantum yield (see Table 1).

It turned out that the number of PcAlCl aggregates in nanostructures can change over time. Thus, in the absorption spectra of an aqueous solution of PcAlCl–CPL5, the optical density of the band at 644 nm increased with time, while the intensity of the band at 683 nm, on the contrary, decreased (Figure S3). This effect can be explained by the formation of stable H-aggregates of PcAlCl with the participation of water with its slow diffusion into the polymer particle or by intermolecular interactions between PcAlCl and monomer units of the terpolymer over time.

It should be noted that the interaction of PcAlCl–copolymer particles with cell membranes and other biological structures can lead to the release of the encapsulated dye and a sharp increase in dye absorbance, fluorescence signal and generation of reactive oxygen species, as was shown in previous work[13] for methyl pheophorbide *a* dye encapsulated in similar copolymer-based NPs.

The size of nanostructures is of great importance for their successful penetration into the cell and accumulation. The optimal NP size for passive targeting due to the ‘enhanced permeability and retention effect’ (EPR effect) may vary depending on the tumor type and corresponds to a diameter of approximately 200 nm.[24,25] We used the DLS method to estimate the size of PcAlCl–copolymer nanostructures dissolved in phosphate-buffered saline. Figure S4 shows the distribution curves of light scattering intensity over the sizes of scattering centers for the corresponding nanostructures. It can be seen that the DLS curves are multimodal for the PcAlCl–CPL1, PcAlCl–CPL2 and PcAlCl–CPL3 nanostructures. In the PcAlCl–CPL1 solution, the main contribution to light scattering comes from particles with a hydrodynamic radius at the peak maxima of *ca*. 57 and 164 nm, while the contribution of smaller particles is higher. The PcAlCl–CPL4 solution is dominated by particles with a size of about 105 nm, while the PcAlCl–CPL2 solution contains larger particles with an R_h of about 474 nm. Meanwhile, the size distribution of scattering centers in PcAlCl–CPL3 and PcAlCl–CPL5 solutions differs significantly: in the first case, they are about 77 nm at the peak maximum, and in the second, 57 nm. Thus, PcAlCl–terpolymer structures fall within the optimal size range for accumulation in tumors via the passive targeting mechanism. The size of PcAlCl–copolymer structures can be controlled by the physicochemical properties of VP copolymers.

Figure S5 shows the FTIR spectra of PcAlCl, PcAlCl–CPL1 and PcAlCl–CPL3 powders. Due to the low concentration of PcAlCl in polymer compositions, even its most intense absorption bands are not visible in the region of 1000–700 cm^{-1}. However, its influence on the absorption band at ~1658 cm^{-1}, attributed to the stretching vibrations of the C=O groups of VP units in CPL1, CPL2 and CPL4, is noticeable. This is manifested in its broadening, a slight shift of the maximum to the region of lower wavenumbers, as well as the redistribution of the intensities of absorption bands in the region of 1290 cm^{-1}. Meanwhile, no such changes were detected in the IR spectrum of PcAlCl–CPL3 [Figure S5(*b*)], which suggests that the dye molecules are localized in regions of the copolymer consisting of low-polarity fragments.

To determine the possible binding centers of PcAlCl with the copolymer, we performed quantum chemical modeling of the complex between the dye molecule and the VP, TEGDM and cyclo-HMA monomer units of copolymers using the DFT method (Figure 3 and Table S2). In the VP, TEGDM and cyclo-HMA units, it is the oxygen atoms that form intermolecular bonds and, first of all, these are strong coordination bonds with Al atoms. According to calculations, the shortest bond is formed with the VP unit, while in the complex with TEGDM it is the weakest, possibly due to steric hindrance. The oxygen atoms, as

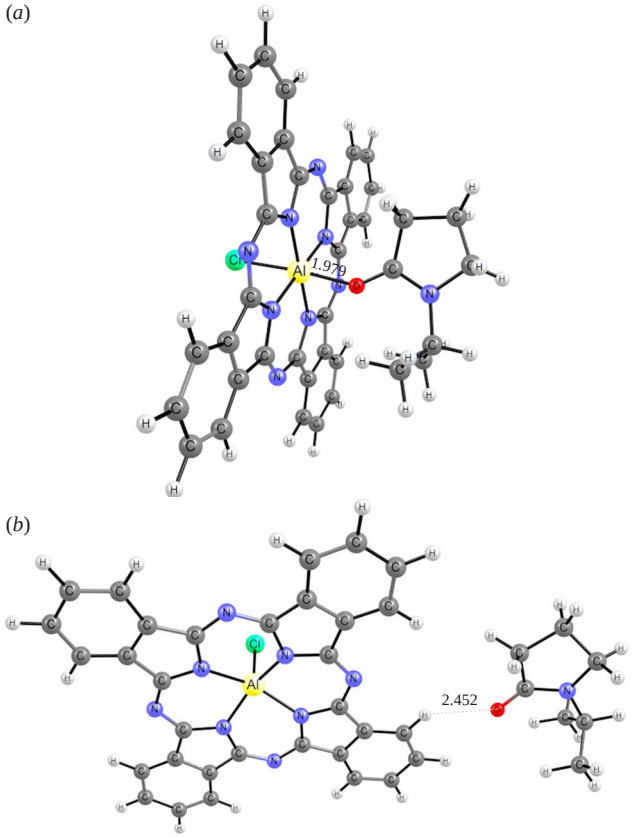

Figure 3 Possible structures of PcAlCl complexes with a VP unit, where the bonding centers in PcAlCl are (*a*) the Al atom and (*b*) the H atom of the C–H bond.

usual, form bonds with the hydrogen atoms of the PcAlCl macrocycle, and their lengths are approximately the same for all monomers. The hydrogen atoms of monomers weakly participate in the formation of bonds with the guest molecule. It was not possible to identify structures with the H···N(PcAlCl) bond because they disintegrated during the optimization process. There are structures with H···Cl(PcAlCl) bonds; however, according to QTAIM calculations, their energy does not exceed 0.5 kcal mol^{-1}. Thus, it can be expected that in polymer structures the PcAlCl molecule will also bind to the corresponding monomer units, forming multiple bonds and intermolecular complexes of varying strength.

The results of this work show that the hydrophobic dye PcAlCl can be solubilized in water by encapsulation in the VP–TEGDM copolymer or VP–PEGMEM–TEGDM and VP–(cyclo-HMA)–TEGDM terpolymers. In their NPs, PcAlCl retains strong absorbance in the red region of the spectrum and fluorescence properties, which depend on the localization of dye molecules in regions of polymer matrices that differ in polarity. Terpolymers enriched in hydrophobic cyclo-HMA units or hydrophobic $SC_{10}H_{21}$ residues are most suitable for reducing dye aggregation. VP copolymers with adjustable parameters and their compositions with the hydrophobic dye can be useful tools for the development of new effective PSs for PDT in the treatment of oncological diseases and microbial infections, as well as for fluorescence diagnostics. Preliminary tests of the studied phthalocyanine–polymer compositions with lecithin liposomes and mouse brain tissue homogenate showed that the dye is transferred from the polymer NPs to the membranes and its fluorescence increases significantly over time. This gives reason to believe that the nanoscale systems developed in this work will also exhibit high phototoxicity.

This work was carried out within the framework of the state assignment (state registration nos. 124013000722-8, 124020500019-2 and 124013000692-4).

Online Supplementary Materials

Supplementary data associated with this article can be found in the online version at doi: 10.1016/j.mencom.2024.06.007.

References

1 A. B. Sorokin, *Chem. Rev.*, 2013, **113**, 8152.
2 M. L'Her and A. Pondaven, in *The Porphyrin Handbook*, eds. K. M. Kadish, K. M. Smith and R. Guilard, Academic Press, San Diego, CA, 2003, vol. 16, pp. 117–169.
3 A. F. Mironov, K. A. Zhdanova and N. A. Bragina, *Russ. Chem. Rev.*, 2018, **87**, 859.
4 A. Escudero, C. Carrillo-Carrión, M. C. Castillejos, E. Romero-Ben, C. Rosales-Barrios and N. Khiar, *Mater. Chem. Front.*, 2021, **5**, 3788.
5 J.-J. Hu, Q. Lei and X.-Z. Zhang, *Prog. Mater. Sci.*, 2020, **114**, 100685.
6 D. A. Bunin, A. G. Martynov, D. A. Gvozdev and Y. G. Gorbunova, *Biophys. Rev.*, 2023, **15**, 983.
7 K. Sztandera, M. Gorzkiewicz and B. Klajnert-Maculewicz, *Wiley Interdiscip. Rev.: Nanomed. Nanobiotechnol.*, 2020, **12**, e1509.
8 S. Pramual, K. Lirdprapamongkol, J. Svasti, M. Bergkvist, V. Jouan-Hureaux, P. Arnoux, C. Frochot, M. Barberi-Heyob and N. Niamsiri, *J. Photochem. Photobiol., B*, 2017, **173**, 12.
9 C. V. Synatschke, T. Nomoto, H. Cabral, M. Förtsch, K. Toh, Y. Matsumoto, K. Miyazaki, A. Hanisch, F. H. Schacher, A. Kishimura, N. Nishiyama, A. H. E. Müller and K. Kataoka, *ACS Nano*, 2014, **8**, 1161.
10 Y. P. Istomin, M. A. Kaplan, S. V. Shliakhtsin, T. P. Lapzevich, D. A. Cerkovsky, L. N. Marchanka, A. S. Fedulov and T. V. Trukhachova, *Proc. SPIE*, 2009, **7380**, 73806V, doi: 10.1117/12.823840.
11 Z. Ouyang, Y. Gao, M. Shen and X. Shi, *Mater. Today Bio*, 2021, **10**, 100111.
12 S. V. Kurmaz, N. V. Fadeeva, A. V. Komendant, V. M. Ignatiev, N. S. Emelyanova, G. V. Shilov, T. S. Stupina, N. V. Filatova, M. A. Lapshina and A. A. Terentyev, *Polym. Bull.*, 2022, **79**, 8905.
13 A. Yu. Rybkin, S. V. Kurmaz, E. A. Urakova, N. V. Filatova, L. R. Sizov, A. V. Kozlov, M. O. Koifman and N. S. Goryachev, *Pharmaceutics*, 2023, **15**, 273.
14 S. V. Kurmaz, N. V. Fadeeva, J. A. Skripets, R. I. Komendant, V. M. Ignatiev, N. S. Emel'yanova, Y. V. Soldatova, I. I. Faingold, D. A. Poletaeva and R. A. Kotelnikova, *Mendeleev Commun.*, 2022, **32**, 117.
15 Y. V. Soldatova, I. I. Faingold, D. A. Poletaeva, A. V. Kozlov, N. S. Emel'yanova, I. I. Khodos, D. A. Chernyaev and S. V. Kurmaz, *Pharmaceutics*, 2023, **15**, 1388.
16 S. V. Kurmaz, I. I. Ivanova, N. V. Fadeeva, V. M. Ignatiev, N. S. Emelyanova, M. A. Lapshina, A. A. Balakina and A. A. Terentiev, *Russ. Chem. Bull.*, 2023, **72**, 1349.
17 S. V. Kurmaz, E. O. Perepelitsina, S. G. Vasiliev, I. A. Avilova, I. I. Khodos, V. A. Kurmaz, D. A. Chernyaev, Y. V. Soldatova, N. V. Filatova and I. I. Faingold, *Int. J. Mol. Sci.*, 2023, **24**, 15170.
18 S. V. Kurmaz, I. I. Ivanova, N. S. Emelyanova, D. V. Konev, V. A. Kurmaz, N. V. Filatova, A. A. Balakina and A. A. Terentiev, *Mendeleev Commun.*, 2023, **33**, 255.
19 É. L. de Oliveira, S. B. S. Ferreira, L. V. de Castro-Hoshino, K. da S. S. Campanholi, I. R. Calori, F. A. P. de Morais, E. Kimura, R. C. da Silva Junior, M. L. Bruschi, F. Sato, N. Hioka and W. Caetano, *Langmuir*, 2021, **37**, 3202.
20 I. R. Calori and A. C. Tedesco, *Dyes Pigm.*, 2020, **173**, 107940.
21 Z. Ou, J. Shen and K. M. Kadish, *Inorg. Chem.*, 2006, **45**, 9569.
22 E. Zenkevich, E. Sagun, V. Knyukshto, A. Shulga, A. Mironov, O. Efremova, R. Bonnett, S. P. Songca and M. Kassem, *J. Photochem. Photobiol., B*, 1996, **33**, 171.
23 D. V. Batov, A. V. Kustov, S. O. Kruchin, V. V. Makarov and D. B. Berezin, *J. Struct. Chem.*, 2019, **60**, 443 (*Zh. Strukt. Khim.*, 2019, **60**, 461).
24 M. Morales-Cruz, Y. Delgado, B. Castillo, C. M. Figueroa, A. M. Molina, A. Torres, M. Milián and K. Griebenow, *Drug Des., Dev. Ther.*, 2019, **13**, 3753.
25 Y. Yang and C. Yu, *Nanomedicine*, 2016, **12**, 317.

Received: 12th March 2024; Com. 24/7422